Novel bilayer dissolving microneedle arrays with concentrated PLGA nano-microparticles for targeted intradermal delivery: Proof of concept

Lalit K. Vora, Ryan F. Donnelly, Eneko Larraneta, Patricia González-Vázquez, Raghu Raj Singh Thakur, Pradeep R. Vavia

PII: S0168-3659(17)30892-1
DOI: doi:10.1016/j.jconrel.2017.10.005
Reference: COREL 8992

To appear in: *Journal of Controlled Release*

Received date: 30 May 2017
Revised date: 25 September 2017
Accepted date: 6 October 2017

Please cite this article as: Lalit K. Vora, Ryan F. Donnelly, Eneko Larraneta, Patricia González-Vázquez, Raghu Raj Singh Thakur, Pradeep R. Vavia , Novel bilayer dissolving microneedle arrays with concentrated PLGA nano-microparticles for targeted intradermal delivery: Proof of concept. The address for the corresponding author was captured as affiliation for all authors. Please check if appropriate. Corel(2017), doi:10.1016/j.jconrel.2017.10.005

Novel bilayer dissolving microneedle arrays with concentrated PLGA nano-microparticles for targeted intradermal delivery: Proof of Concept

Lalit K. Vora[a,b], Ryan F. Donnelly[a], Eneko Larraneta[a], Patricia González-Vázquez[a], Raghu Raj Singh Thakur[a], Pradeep R. Vavia[b]*

a.School of Pharmacy, Queen's University Belfast, 97 Lisburn Road, Belfast BT9 7BL, UK

b. Department of Pharmaceutical Sciences and Technology, Institute of Chemical Technology, University Under Section 3 of UGC Act – 1956, Elite Status and Center of Excellence, Govt. of Maharashtra, Mumbai 400 019, India

Abstract

Polymeric microneedle (MN) arrays continue to receive growing attention due to their ability to bypass the skin's *stratum corneum* barrier in a minimally-invasive fashion and achieve enhanced transdermal drug delivery and "targeted" intradermal vaccine administration. In this research work, we fabricated biodegradable bilayer MN arrays containing nano - microparticles for targeted and sustained intradermal drug delivery. For this study, model drug (vitamin D_3, VD_3)-loaded PLGA nano- and microparticles (NMP) were prepared by a single emulsion solvent evaporation method with 72.8% encapsulation of VD_3. The prepared NMP were directly mixed 20% w/v poly(vinyl pyrrolidone) (PVP) gel, with the mixture filled into laser engineered micromoulds by high-speed centrifugation (30 min) to concentrate NMP into MN shafts. The particle size of PLGA NMP ranged from 300 nm to 3.5 μm and they retained their particle size after moulding of bilayer MN arrays. The relatively wide particle size distribution of PLGA NMP was shown to be important in producing a compact structure in bilayer conical, as well as pyramidal, MN, as confirmed by scanning electron microscopy. The drug release profile from PLGA NMP was tri-phasic, being sustained over 5 days. The height of bilayer MN arrays was influenced by the weight ratio of NMP and 20% w/v PVP. Good mechanical and insertion profiles (into a skin simulant and excised neonatal porcine skin) were confirmed by texture analysis and optical coherence tomography, respectively. *Ex vivo* intradermal neonatal porcine skin penetration of VD_3 NMP from bilayer MN was quantitatively analysed after cryostatic skin sectioning, with 74.2 ± 9.18% of VD_3 loading delivered intradermally. The two-stage novel processing strategy developed here provides a simple and easy method for localising particulate delivery systems into dissolving MN. Such systems may serve as promising means for controlled transdermal delivery and targeted intradermal administration.

Keywords: Microneedles, Bilayer, PLGA, Nanoparticles, Microparticles, Vitamin D_3

1. Introduction

Transdermal drug delivery is a useful approach for administration of therapeutic molecules, as it bypasses first-pass metabolism associated with oral administration [1]. However, the molecules which can be delivered *via* the transdermal route are restricted to small (<500 Da) and moderately hydrophobic agents, due to the *stratum corneum*, which is the foremost barrier to systemic absorption of topically-applied drugs [2-4]. To improve delivery across the *stratum corneum*, a range of physical enhancement methods have been developed, including iontophoresis [4], ultrasound [5], liquid jet injection [6], gene guns [7], laser [8] and electroporation [9], all with relatively limited success [10]. Micron-scale needles (10 μm -900 μm), called microneedles (MN) [11, 12], represent a much more promising approach.

MN are minimally-invasive, pain-free devices capable of penetrating the skin's *stratum corneum*, thereby overcoming its barrier properties [13]. Therefore, MN platforms can potentially provide rapid or controlled transdermal delivery for an increased number of therapeutic molecules [14]. MN technology is, at last, realizing its early promise, with human trials recently conducted for the delivery of vaccines using dissolving MN patches [15]. There is a now the possibility to deliver molecules as a bolus dose using rapidly-dissolving MN and also to achieve longer-term controlled transdermal delivery through encapsulation of drugs prior to MN formulation or direct loading into biodegradable MN. For such sustained delivery applications, MN patches may need to remain inserted in skin for hours or even days. Such prolonged insertion times could cause as-yet unseen problems. To prevent this, several approaches have been developed for long-term controlled transdermal delivery, including the use of solid MN to generate physical pores in *stratum corneum* prior to topical application of controlled release particle suspensions or rapid delivery of drug-loaded polymer particles into the skin by dissolving microneedle arrays. Considering the pore sized generated by MN puncture, as well as the area of the *stratum corneum* typically treatable using conventional MN patches, achieving a clinically-relevant effect would be difficult to achieve for all but the most potent therapeutic agents [16]. Improved designs could enhance patient care.

Dissolving polymeric MN are a potential choice for targeted transdermal and intradermal delivery because of their simple and readily-scalable fabrication and low cost [17]. Recently, dissolving MNs have proved to augment transdermal and intradermal delivery of a variety of hydrophilic molecules, particularly bio-macromolecules [18].

Various biodegradable and water-soluble polymers have been used to fabricate dissolving MN arrays for rapid drug delivery [19]. However, developing biodegradable nano-microparticles loaded dissolving MN arrays, in which the release rate could be controlled may be useful for a variety of molecules [20].

Poly(lactic-co-glycolic acid) (PLGA) is the most explored polymer for nanoparticle and microparticle design for targeted and controlled drug delivery systems due to its biodegradability and good biocompatibility [21]. PLGA carriers provide controlled drug release from periods of a few days up to several months based on their molecular weight and ratio of lactide: glycolide chains. PLGA degrades into water-soluble, non-toxic, products through hydrolysis *in-vivo*. Indeed, several PLGA microparticle-based products, such as Lupron Depot®, are currently approved for human use [22].

In this paper, we present a simple yet innovative technique to prepare two-layered MN arrays to improve the intradermal delivery of nanoparticles and microparticles. For this purpose, vitamin D_3 (VD_3) was selected as a model drug. First, VD_3 was encapsulated within PLGA nano-microparticles (NMP) by an emulsion solvent evaporation method. NMP were characterised for particle size, encapsulation efficiency and release profile and, subsequently, loaded inside the needle tips of MN arrays by single-step centrifugation. The developed bilayer MN system was tested for *ex-vivo* intradermal neonatal porcine skin penetration by optical coherence tomography and cryostat microtome skin sectioning and drug deposition was quantified.

2. **Materials & methods**

2.1. Materials

Vitamin D_3, D-α-tocopherol succinate and PLGA Resomer 752H (molecular ratio of D,L-lactide/glycolide 75/25, Mw 9850 g/mol), poly(vinylpyrrolidone) (PVP, MW 360,000 g/mol) and poly(vinyl alcohol) (PVA, MW 10000 g/mol), acetonitrile and methanol (both of HPLC grade) were all purchased from Sigma-Aldrich (Poole, Dorset, UK). Parafilm M@, a flexible thermoplastic sheet (127 µm thickness) made of olefin-type material and used as a skin simulant for insertion studies, was obtained from BRAND GMBH (Wertheim, Germany). All other chemicals used were of analytical grade. Millipore HPLC-grade water was used throughout the study.

2.2. Preparation of PLGA nano-microparticles

PLGA NMP were prepared using an oil-in-water (O/W) emulsion solvent evaporation method. Briefly; PLGA (100 mg) and model drug, VD_3 (25 mg) with stabiliser, tocopherol succinate (TS) (10 mg), were dissolved in 1 ml of methylene chloride (DCM). This organic phase was added into 3 ml cooled double distilled water containing 2% w/v PVA, with or without 5% w/v mannitol. The resulting mixture was subjected to homogenisation at 18,000 rpm for 60 sec using a high-speed homogenizer (Yellowline ID18 Basic, IKA, Brazil) in order to produce a stable o/w emulsion with diminished droplet size. The organic solvent was then removed by evaporating under magnetic stirring for 3 h at room temperature to yield solid NMP. The particle size was measured using a Mastersizer 3000 (Malvern, Worcester, UK). To check entrapment efficiency and other solid state characteristics of the prepared NMP, the entire dispersion was centrifuged at 11,000 rpm for 10 min using a high-speed centrifuge in three cycles and the sediment constituting NMP was removed. NMP were then pre-frozen (-70 °C) for 12 h and subsequently lyophilized for 8 h with hold and ramp cycles from -40 °C to 25°C.

2.3. Fabrication of PLGA particles loaded dissolving bilayer microneedles

The fabrication of MN arrays containing PLGA NMP is summarised in Figure 1. Briefly, NMP in 2% w/w PVA were mixed with equal weights of 20% w/v aqueous solution of PVP (Mw~ 360 kDa) and approximately 500 mg of this mixture was poured into laser-engineered silicone conical (19×19 and 12×12 arrays) as well as master-templated pyramidal (14×14 arrays) micromould templates [17]. All these moulds showed needle heights of 600 µm and widths at base of 300 µm. The moulds were centrifuged at 2913×g for 30 min and then allowed to dry under ambient condition for 48 hours. To optimize the NMP concentration in needles of the dissolving MN array, different weight ratios of NMP and 20% w/v PVP were investigated, as summarized in Table 1. MN arrays were then removed from the moulds and assessed for needle formation and mechanical strength**.** For use as a control in permeation studies, MN-free control patches were prepared by the same method, except using micromoulds with no indentations.

2.4.Particle characterisation

Particle size and polydispersity of NMP before and after MN formulation were evaluated on the Mastersizer 3000. Around 20 mg of hydrated NMP were suspended in deionized water

and stirred at 1700 rpm. In order to determine particle size, each sample was measured 6 times. The dispersant and particle refractive index (RI) were 1.33 and 1.59, respectively. Similarly, the particle size of NMP was measured after incorporating into MN arrays by dissolving the arrays in 15 ml phosphate-buffered saline (pH 7.4). Subsequently, 5 ml of this solution was added into 500 ml of distilled water and the particle size was measured.

2.5. Drug content analysis

The content of the VD_3 in the PLGA NMP was determined by disruption of accurately weighed 5 mg NMP using 0.2 ml of acetonitrile. After dissolving NMP in acetonitrile by vortexing, 0.8 ml methanol was added to precipitate the PLGA polymer while VD_3 remained soluble in the acetonitrile-methanol mixture. The disrupted NMP solution was then centrifuged at 10,000 rpm for 5 minutes and the total VD_3 content was determined using HPLC (see Section 2.7). The percentage of the VD_3 entrapped was calculated as follows:

$$\text{Entrapment efficiency (\%)} = \frac{\text{Amount of drug entrapped}}{\text{Total amount of drug taken}} \text{ x } 100 \qquad \text{Eq. 1}$$

To determine total content VD_3 in bilayer MN arrays, only tips of MN arrays without baseplate were removed carefully using a scalpel and placed into Eppendorf tubes to determine VD_3 content as per the above procedure. These experiments performed in triplicate.

2.6. In-vitro release of drug from PLGA NMP

Accurately 15 mg of freeze-dried PLGA NMP were placed in a 2 ml microcentrifuge tube and suspended in 1 ml of 10 mM PBS pH 7.4 with 1% w/v Tween 80 [23]. This mixture was kept under stirring at 50 rpm in a waterbath shaker at 37 ± 2ºC. At predetermined time intervals, samples were collected and centrifuged at 3000 rpm for 5 min. Aliquots of 1 ml supernatant were taken and replaced with an equal volume of fresh release medium. The supernatant was centrifuged at 10,000 rpm for 10 min. The amount of drug in the collected supernatant was measured by HPLC. All release tests were performed in triplicate over 7 days.

2.7. Pharmaceutical Analysis

Quantification of VD_3 was performed using reversed-phase HPLC (Agilent 1200® Binary Pump, Agilent 1200®, Standard Autosampler, Agilent 1200® Variable Wavelength Detector; Agilent Technologies UK Ltd., Stockport, UK). Chromatographic separation was achieved using a Luna C_{18} (ODS1) column (150 × 4.6 mm^2 i.d. with 5 µm packing; Phenomenex, Macclesfield, UK) with isocratic elution and UV detection at 265 nm. The mobile phase was a mixture of acetonitrile: methanol: water (90:08:02 v/v/v) with a run time of 8 min**.** The column temperature was 20°C and the injection volume was 20 µL. The chromatograms obtained were analysed using Agilent ChemStation Software B.02.01.

2.8. Microscopy analysis of MN arrays

Surface morphology of PLGA NMP-loaded MN arrays was evaluated by using optical and scanning electron microscopy. A Keyence VHX-700F Digital Microscope (Keyence, Osaka, Japan) and a TM3030 benchtop scanning electron microscope (SEM) (Hitachi, Tabletop Microscope, Europe) were used. The latter was used in low vacuum mode at a voltage of 15 kV.

2.9. Mechanical and insertion properties of NMP loaded MN arrays

To assess the compression and insertion properties of the bilayer MN arrays, a mechanical test was conducted using a TA-XT2 Texture Analyser (Stable Microsystems, Haslemere, UK) in compression mode, as described previously [24]. To test compression, the initial heights of bilayer MN arrays were first determined by using a stereomicroscope. Then, bilayer MN arrays were attached with the help of double-sided adhesive tape to the movable cylindrical probe of the Texture Analyser and pressed by the test station against a flat aluminium block at a rate of 1.19 mm/s for 30 s and a force of 32 N. These force conditions approximately replicate the average conditions of patients applying MN arrays, as described previously [25].

Bilayer MN heights were measured again using the stereomicroscope and the percentage reductions in height following the application of the axial compression load were calculated. To determine insertion properties, Parafilm M® was used as per previously validated insertion model [26]. The initial heights of the bilayer MN arrays were measured microscopically prior to this test. The Parafilm M® sheet was folded into an eight-layer film (approximately 1 mm thickness). Following attachment of the MN array to the movable probe of the Texture Analyser, the probe was lowered onto the folded Parafilm M® at a speed of 1.19 mm/s until

the required force of 32 N was exerted and held for 30 s. The MN were then removed from the Parafilm M® sheet after insertion, the sheet unfolded and the number of holes in each layer and MN heights evaluated using a Leica EZ4 D digital microscope (Leica, Wetzlar, Germany).

2.10. Optical Coherence Tomography

Eight layers of Parafilm M® (≈1 mm thickness) was used as a skin simulant for MN insertion studies. Neonatal porcine full-thickness skin was also used to check insertion of NMP loaded MN tips. MN arrays were inserted using the Texture Analyser, with force of 32 N for 30 s. Optical coherence tomography (OCT) images were recorded using an EX1301 OCT Microscope (Michelson Diagnostics Ltd., Kent, UK).

2.11. Ex-vivo deposition studies in excised porcine skin

Ex-vivo deposition of VD_3 loaded PLGA NMP containing bilayer MN was performed in the excised porcine skin as per previously reported procedures [27]. In detail, the receptor compartment of standard jacketed Franz-type diffusion cell was filled with degassed PBS pH 7.4 and was thermostatically controlled at 37 °C. Full thickness neonatal porcine skin was excised from stillborn piglets, shaved and pre-equilibrated in PBS pH 7.4 for 1 h before beginning the experiments. A circular specimen of the skin was secured to the donor compartment of the diffusion cell using cyanoacrylate adhesive with the *stratum corneum* side facing the donor compartment. Bilayer MN arrays were inserted using manual pressure. MN-free control patches were similarly applied. After 6 h of the application period, the skin sample was removed and separated from the MN array. The surface of the specimen was carefully wiped with a damp tissue to remove any traces of the formulation. A circular-shaped scalpel was used to excise the tissue exposed to the MN array, which was then flash frozen in a liquid nitrogen atmosphere prior to tissue sectioning. Sections of frozen tissue were fixed on the stage of a cryostatic microtome (Leica CM1900-1-1 cryostatic microtome, Leica Microsystems, Nussloch, Germany) using tissue embedding fluid. The microtome environment and stage were operated at -25 °C. Frozen tissue sections were positioned so that their upper surfaces, to which patches had been attached, were parallel to the sliding motion of the blade. Slice thickness was set at 50 µm and 4 consecutive slices were taken and placed into 1.5 ml Eppendorf tubes. This procedure was repeated until the entire section was

sliced. The total depth of slicing into the tissue was approximately 1.5 mm. To the Eppendorf tubes, 1 ml of acetonitrile was added and sonicated for 30 min. Samples were then centrifuged at 10,000 rpm for 5 min and the supernatant containing extracted drug was collected and quantified using HPLC.

2.12. Statistical analysis

The results are presented as means ± standard deviation (SD) of the mean. Statistical comparison between bilayer MN and control patches, in terms of depth penetration, were made using the Mann-Whitney U-test by using GraphPad Prism software (ver. 6; GraphPad, Inc., San Diego, USA). A difference of $p < 0.05$ was considered to be statistically significant.

3. Results

3.1 Characterisation of VD_3 loaded PLGA NMP

In this study, the PLGA NMP were prepared using a single emulsion method. Particle size was found to range from nano to micron scale, with a relatively wide particle size distribution, as shown in Figure 2. Particle size of NMP prepared with mannitol (D 10: 386 nm, D 50: 920 nm, D 90: 2.74 µm with span value 2.55) (Figure 2 B) was found to be slightly lower than NMP prepared without mannitol (D 10: 409 nm, D 50: 1007 nm, D 90: 3.55 µm with span value 2.92) (Figure 2 A). Formulations containing mannitol with PVA as an osmotic agent exhibited improved drug encapsulation (from 59.85% to 72.8%). A NMP loading of VD_3 of 133 ± 24 µg/mg was achieved with mannitol. Here, the single emulsion was prepared at higher speed (18,000 rpm) to get broader particle sizes with high span value. This wider particle size distribution was a prerequisite to achieving tightly packed particles in MN tips as discussed further later. The PLGA NMP exhibited a negative zeta-potential of -27.2 ± 0.69 mV.

3.2 In-vitro release study

Real-time drug release kinetics of VD_3 from PLGA NMP exhibited a typical tri-phasic release profile up to 5 days, as shown in Figure 3. An initial burst release followed by a slower release can be observed. Finally, a third release phase was observed, due to the broad particle size distribution from nano- to micron size of PLGA particles. The PLGA NMP prepared in the presence of mannitol showed a slightly lower initial burst release compared to the PLGA microspheres prepared alone in PVA solutions. Mannitol acts as an osmotic, agent giving a less porous NMP structure. Hence, we observed that mannitol-added NMP showed a drug

release of over 13% at the first hour, whereas the NMP batch without the addition of mannitol showed 22 % drug release. As the initial burst release is governed by a diffusion mechanism, less porous NMP structure prepared with mannitol gives lower diffusion-based burst release.

3.3 Characteristics of PLGA NMP loaded PVP MN arrays

The digital microscopic images (Figure 4) clearly showed NMP specifically concentrated at the tips (white in colour) of MN arrays. Accumulation of NMP in the MN tips was due to the high density of PLGA particles (1.3g/cm^3) [26] and the use of high-speed centrifugation during MN preparation. The resulting needles measured 600 μm in height with PLGA particle concentrated sharp tips tapering to a 20 μm radius of curvature that encapsulated 265 ± 32 μg (n=3) of VD_3 per patch (0.49cm^2 size). Heights of bilayer MN with PLGA NMP were customised by different weight ratios of NMP to PVP polymer gel, as shown in Figure 5. As particle size is a vitally-important stability parameter for NMP, particle size was measured before and after MN preparation. The PLGA NMP embedded bilayer MN was dissolved in PBS pH 7.4 buffer without any changes in particle size or observation of aggregation. The average particle size remained similar before and after making MN, as shown in Table 2. Here, the dried state of the polymer matrix of MN possibly acts as a stabiliser for NMP particle size.

3.4 Scanning Electron Microscopy

To further characterise the MN, the structures were examined using SEM (Figure 6). SEM images showed NMP specifically concentrated in MN tips and compactly packed. The different particle sizes from nano to micron size level in addition to the presence of adhesive PVP polymer gave a compactly packed structure to the arrays. The tips of bilayer MNs were packed with PLGA NMP with a porous structure. There was a discrete line between PLGA NMP mixed with PVP polymer and plain PVP polymeric matrix clearly visible (figure 6.Ai). There was a porous and rough texture at the tips of MN containing PLGA particles, while a smoother texture was exhibited by the unloaded PVP microneedles. These topographies could reflect different arrangements of the incorporated PLGA particles within the matrix of PVP polymer. To study the structure of the interior of tips of the MN, they were broken and then visualised by SEM. We found that the interior of the tips of the MN was also completely and compactly filled with PLGA particles in the PVP matrix. (Figure. 6B). Microparticles and

nanoparticles were spherical with a similar size measured by SEM as that measured using the particle sizer.

3.5 Mechanical strength and Parafilm insertion of MN arrays

Following application of the axial load, the bilayer MN showed a 10.77% height reduction (Figure 7B). The mechanical strength of MN arrays was found to be strong enough to bear 32 N force used for skin and Parafilm M® insertion. The same force of 32 N was applied to assess the effects of insertion on needle height, using Parafilm M® as an artificial membrane to mimic the skin [26]. It was found that NMP loaded bilayer MN penetrated to the third layer of Parafilm M® (Figure 7A). Considering the thickness of each layer of the Parafilm M® membrane (127 μm), the insertion depth could be measured up to 381 μm which relates to more than 60% of the needle height inserted.

3.6 Determination of skin penetration

A non-invasive optical imaging technique, OCT, was used to acquire real-time images of the insertion of the bilayer dissolving MN patches in the neonatal porcine skin and Parafilm M® layers. The two-dimensional side-view of bilayer MNs inserted into the porcine skin are shown in Figure 8B. Bilayer MN patches possessed the capability to be inserted into neonatal porcine skin, reaching insertion depths of approximately 250–300 μm. In the case of Parafilm M®, it was penetrated down to the third layer (approximately 370 μm), as shown in Figure 8A. This is very similar to previous insertion studies of polymeric MN into Parafilm M® [27].

3.7 Ex-vivo deposition studies in excised porcine skin

Deposition of VD_3 across neonatal porcine skin was significantly enhanced by using bilayer MN arrays in comparison with the control set-up ($p < 0.05$) (Figure 9). As can be seen in the drug permeation profile, drug concentration increased with skin depth, until reaching a maximum at a depth of 0.4 mm (171.7 ± 7.39μg/cm^2). The concentration of VD_3 in deeper layers of the skin (depths between 0.4 mm and 1.4 mm) was lower. Negligible in-skin drug concentrations in the case of control VD_3-NMP loaded patch films were found. Considering the cumulative concentration of VD_3 in the skin after MN insertion, 74.2 ± 9.18% (196.6 ± 24.3 μg) of VD_3 of the initial amount of the drug present in the array was administered. These results are in close agreement with the insertion studies described previously [28]. Therefore,

the results demonstrate the bilayer PVP-based dissolving MN arrays significantly assist the delivery of the drug particles into skin. Such particles may then sustain delivery long after the MN patches are removed from skin.

Discussion

MN technology has been used to enhance skin permeability to nanoparticles and microparticles. Several studies can be found in the literature describing MN-assisted permeation of nano- and micro-metric particles [29]. PLGA- and PLA-based biodegradable MN were prepared for controlled and/or targeted skin delivery. These polymers are well explored and extensively characterised for targeted and controlled drug delivery because of the biodegradable nature of PLGA. Tailored drug release can be achieved based on its molecular weight and lactide: glycolide ratio [30]. However, the formulation process requires the use of organic solvents and/or elevated temperatures that can damage biomolecule stability [31]. Besides, it is difficult to load high doses of drug or drug-loaded particles in MN tips. Some researchers have performed multiple steps to concentrate the particles in the needle tips [32]. To construct MN arrays capable of rapid delivery of drug-loaded PLGA particulate cargos, we developed bilayer MN to deposit PLGA NMP into the viable layers of the skin upon the aqueous dissolution of a supportive PVP polymer matrix. The proposed method to concentrate the NMP in the MN tips only required a single centrifugation step. Using this technique, it is possible to concentrate the drug-loaded polymeric particles into the MN tips for intradermal delivery without wastage of drug. We postulated that such a platform would provide rapid administration through short time MN application, while facilitating combined bolus and long-term dosing of cargos released from cutaneous implantation of PLGA nano- and microparticulate depots, respectively.

VD_3 was selected as a model drug to prove this concept with PLGA NMP. This molecule is hydrophobic and potent. These two characteristics make this drug an ideal candidate for this study, as it can be easily encapsulated in hydrophobic PLGA nanoparticles. The potency of the drug is important because the drug loading in the MN arrays is limited, as the drug is encapsulated inside NMP and subsequently incorporated into the needle tips.

Firstly, VD_3 loaded PLGA NMP were prepared and characterized for particle size and encapsulation. The release kinetics of the drug from the PLGA particles was evaluated as the drug can be released in different ways based on the particle size [33]. *In-vitro* release kinetics

of VD_3 from PLGA NMP exhibited a typical tri-phasic release profile. A tri-phasic release phenomenon has been found when a lag release period occurs after the initial burst from nanoparticles and the surfaces of microparticles and until polymer degradation starts in the microparticles. Therefore, the combined range of nano and micron size particles is used here as an advantage to tailor immediate and then sustained drug release, respectively.

PVP was selected as the mechanical and structural material for dissolving MN with PLGA NMP, as it exhibits high water solubility with good mechanical strength and is biocompatible [34, 35]. Concentrated PLGA particles at the tips of MN arrays remained together because of the very good adhesive properties of the PVP polymer. Moreover, this type of MN array could be prepared successfully using different micromould shapes, like pyramidal and conical shapes (Figures 4 and 6). PLGA NMP preparation was carried out in a PVA solution because of its surfactant and stabiliser effects during the single emulsion solvent evaporation method. PVA is a well-established polymeric surfactant for PLGA nanoparticle and microparticle preparation [36]. The prepared PLGA NMP prepared with PVA were directly mixed with PVP gels for MN preparation. Here, advantageously, there was no need to dry the NMP by lyophilisation before MN formulation. MN prepared from pure PVP were brittle in nature [20] and low molecular weight PVA acted as a softening agent to yield good mechanical properties in PVP MN.

Herein, the wider particle size distribution of NMP as shown in Figure 3 and Table 1 was advantageously used to achieve compact packaging of NMP into MN tips (similar to the sand-pebble mixture in the bottle to fill it completely without any voids). It was quite possible to preferentially accumulate PLGA NMP in tips because of the high density of PLGA particles and the high centrifugation force, as depicted in SEM images in Figure 6. Concentrating the drug particles in the MN tips in this way will, in all, likelihood improve the efficiency of particle deposition in the viable skin layers upon insertion.

As illustrated in the Graphical Abstract, the rationale behind this system is to enable targeted delivery of VD_3-loaded NMP into selected tissues of the skin using soluble PVP MNs. The extracellular fluid of the epidermis and dermis allow dissolution of MN, followed by slow degradation of PLGA, thereby providing sustained delivery of VD_3. This slow release of VD_3 in the epidermis and dermis may mimic the natural sunlight-based VD_3 biosynthesis. *Ex-vivo* deposition studies showed enhanced administration compared to control patches without MN.

VD_3 has been successfully formulated and administrated transdermally and subcutaneously by using different vehicles, including nanocarriers [37-39]. However, our proposed system presents a potential advantage, which is reduction of the administration frequency. In this case, the administration of the MN arrays delivers the vitamin-loaded NMP inside the skin. Subsequently, the particles provide a slow and prolonged release of the molecule over time, thus potentially reducing the frequency of VD_3 administration.

This research work showed an alternative method to prepare and administer PLGA particulate systems with MN-based minimally invasive technology. MN arrays loaded with concentrated NMP allows targeting to the deeper layers of skin for sustained delivery. It is possible that, customisation of molecular weight of polymers and size of particles will permit tailored delivery profiles of molecules based on their desired pharmacological effect. Currently, more than 12 marketed products based on microparticle-based depots of potent molecules exist. These completely rely on subcutaneous or intramuscular injections in clinical setting while MN arrays can be easily self-administered by the patient [40-42]. This type of technology shows potential to be used to sustain delivery of drugs to patients without the use of hypodermic needles and intervention of healthcare professionals. Further studies should now be conducted to evaluate the *in vivo* efficacy of this system. Following this, work on scaled-up manufacture and development of the larger patch sizes required for successful human dosing will be the vital next steps in translation.

5. Conclusions

This study demonstrated a model drug loaded PLGA NMP which specifically was concentrated at the tips of MN arrays to form bilayer dissolving MN structures by a simple centrifugation technique that is commonly used for MN preparation. It was demonstrated that biodegradable nano-microparticles embedded bilayer MN arrays significantly assist skin deposition. These proof-of-concept findings may address the long-standing question of effectively delivering the nanoparticles and microparticles to the viable skin (epidermis and dermis) layers for maximum therapeutic gain and patient compliance.

6. Acknowledgements

We acknowledge financial support from the British Council, United Kingdom, and the Department of Biotechnology, India, under the Newton-Bhabha fund. This research was also supported by The Wellcome Trust (WT094085MA).

7. References

[1] E.S. Khafagy, M. Morishita, Y. Onuki, K. Takayama, Current challenges in non-invasive insulin delivery systems: a comparative review, Adv. Drug Deliv. Rev. 59 (2007) 1521–1546.

[2] S. Coulman, C. Allender, J. Birchall, Microneedles and Other Physical Methods for Overcoming the Stratum Corneum Barrier for Cutaneous Gene Therapy., Crit. Rev. Ther. Drug. Carrier. Syst. 23 (2006) 205-258.

[3] M.J. Garland, K. Migalska, T.M.T. Mahmood, T.R.R. Singh, D. Woolfson, R.F. Donnelly, Microneedle arrays as medical devices for enhanced transdermal drug delivery, Expert Rev. Med. Devices. 8 (2011) 459–482.

[4] Y.N. Kalia, A. Naik, J. Garrison, R.H. Guy, Iontophoretic drug delivery, Adv. Drug Deliv. Rev. 56 (2004) 619–658.

[5] S.E. Lee, K.J. Choi, G.K. Menon, H.J. Kim, E.H. Choi, S.K. Ahn, S.H. Lee, Penetration pathways induced by low-frequency sonophoresis with physical and chemical enhancers: iron oxide nanoparticles versus lanthanum nitrates, J. Invest. Dermatol. 130 (2010) 1063–1072.

[6] D. Sawamura, S. Ina, K. Itai, X. Meng, Kon, K. Tamai, K. Hanada, I. Hashimoto, In vivo gene introduction into keratinocytes using jet injection, Gene Ther. 6 (1999) 1785–1787.

[7] M. Kendall, T. Mitchell, P. Wrighton-Smith, Intradermal ballistic delivery of micro-particles into excised human skin for pharmaceutical applications, J. Biomech. 37 (2004) 1733–1741.

[8] W.R. Lee, S.C. Shen, K.H. Wang, C.H. Hu, J.Y. Fang, The effect of laser treatment on skin to enhance and control transdermal delivery of 5-fluorouracil, J. Pharm. Sci. 91 (2002) 1613–1626.

[9] S.M. Becker, A.V. Kuznetsov, Thermal in vivo skin electroporation pore development and charged macromolecule transdermal delivery: A numerical study of the influence of chemically enhanced lower lipid phase transition temperatures, Int. J. Heat Mass Transf. 51 (2008) 2060–2074.

[10] S. Jain, N. Patel, M.K. Shah, P. Khatri, N. Vora, Recent advances in lipid-based vesicles and particulate carriers for topical and transdermal application, J. Pharm. Sci. 106 (2017) 423–445.

[11] M.R. Prausnitz, Microneedles for transdermal drug delivery, Adv. Drug Deliv. Rev. 56 (2004) 581–587.

[12] S. Kaushik, H. Hord, D.D. Denson, D.V. McAllister, S. Smitra, M.G. Allen, M.R. Prausnitz, Lack of pain associated with microfabricated microneedles, Anesth. Analg. 92 (2001) 502–504.

[13] M.C. Kearney, E. Caffarel-Salvador, S.J. Fallows, H.O. McCarthy, R.F. Donnelly, Microneedle-mediated delivery of donepezil: Potential for improved treatment options in Alzheimer's disease, Eur. J. Pharm. Biopharm. 103 (2016) 43–50.

[14] S. Hirobe, H. Azukizawa, T. Hanafusa, K. Matsuo, Y.S. Quan, F. Kamiyama, I. Katayama, N. Okada, S. Nakagawa, Clinical study and stability assessment of a novel transcutaneous influenza vaccination using a dissolving microneedle patch, Biomaterials. 57 (2015) 50–58.

[15] L.Y. Chu, S.O. Choi, M.R. Prausnitz, Fabrication of dissolving polymer microneedles for controlled drug encapsulation and delivery: Bubble and pedestal microneedle designs, J. Pharm. Sci. 99 (2010) 4228-4238.

[16] P.C. Demuth, W.F. Garcia-Beltran, M.L. Ai-Ling, P.T. Hammond, D.J. Irvine, Composite dissolving microneedles for coordinated control of antigen and adjuvant delivery kinetics in transcutaneous vaccination, Adv. Funct. Mater. 23 (2013) 161–172.

[17] R.F. Donnelly, R. Majithiya, T.R.R. Singh, D.I.J. Morrow, M.J. Garland, Y.K. Demir, K. Migalska, E. Ryan, D. Gillen, C.J. Scott, A.D. Woolfson, Design, optimization and characterisation of polymeric microneedle arrays prepared by a novel laser-based micromoulding technique, Pharm. Res. 28 (2011) 41–57.

[18] M.J. Garland, E. Caffarel-Salvador, K. Migalska, A.D. Woolfson, R.F. Donnelly, Dissolving polymeric microneedle arrays for electrically assisted transdermal drug delivery, J. Control. Release. 159 (2012) 52–59.

[19] H.L. Quinn, E. Larrañeta, R.F. Donnelly, Dissolving microneedles: safety considerations and future perspectives, Ther. Deliv. 7 (2016) 283-285.

[20] I.C. Lee, J.S. He, M.T. Tsai, K.C. Lin, Fabrication of a novel partially dissolving polymer microneedle patch for transdermal drug delivery, J. Mater. Chem. B. 3 (2015) 276–285.

[21] G. Schliecker, C. Schmidt, S. Fuchs, R. Wombacher, T. Kissel, Hydrolytic degradation of poly(lactide-co-glycolide) films: Effect of oligomers on degradation rate and crystallinity, Int. J. Pharm. 266 (2003) 39–49.

[22] S. Fredenberg, M. Wahlgren, M. Reslow, A. Axelsson, The mechanisms of drug release in poly(lactic-co-glycolic acid)-based drug delivery systems-a review, Int. J. Pharm. 415 (2011) 34–52.

[23] S.H. Choi, T.G. Park, Hydrophobic ion pair formation between leuprolide and sodium oleate for sustained release from biodegradable polymeric microspheres, Int. J. Pharm. 203 (2000) 193–202.

[24] H.L. Quinn, L. Bonham, C.M. Hughes, R.F. Donnelly, Design of a dissolving microneedle platform for transdermal delivery of a fixed-dose combination of cardiovascular drugs, J. Pharm. Sci. 104 (2015) 3490–3500.

[25] R.E.M. Lutton, E.Larrañeta, M.C. Kearney, P. Boyd, A.D. Woolfson, R.F. Donnelly, A novel scalable manufacturing process for the production of hydrogel-forming microneedle arrays, Int. J. Pharm. 494 (2015) 417-429.

[26] PLGA (poly lactic-co-glycolic acid) uniform dry microspheres, http://www.polysciences.com/skin/frontend/default/polysciences/pdf/TDS%20858.pdf (Accessed 25.03.17).

[27] E. Larrañeta, J. Moore, E.M. Vicente-Pérez, P. González-Vázquez, R. Lutton, A.D. Woolfson, R.F. Donnelly, A proposed model membrane and test method for microneedle insertion studies, Int. J. Pharm. 472 (2014) 65–73.

[28] R.F. Donnelly, D.I.J. Morrow, F. Fay, C.J. Scott, S. Abdelghany, R.R.T. Singh, M.J. Garland, A.D. Woolfson, Microneedle-mediated intradermal nanoparticle delivery: Potential for enhanced local administration of hydrophobic pre-formed photosensitisers, Photodiagnosis Photodyn, Ther. 7 (2010) 222–231.

[29] E. Larrañeta, M.T.C. McCrudden, A.J. Courtenay, R.F. Donnelly, Microneedles: A new frontier in nanomedicine delivery, Pharm. Res. 33 (2016) 1055–1073.

[30] J. Panyam, M.M. Dali, S.K. Sahoo, W. Ma, S.S. Chakravarthi, G.L. Amidon, R.J. Levy, V. Labhasetwar, Polymer degradation and in vitro release of a model protein from poly(D,L-lactide-co-glycolide) nano- and microparticles, J. Control. Release. 92 (2003) 173–187.

[31] J.H. Park, M.G. Allen, M.R. Prausnitz, Biodegradable polymer microneedles: Fabrication, mechanics and transdermal drug delivery, J. Control. Release. 104 (2005) 51–66.

[32] C. Wang, Y. Ye, G.M. Hochu, H. Sadeghifar, Z. Gu, Enhanced cancer immunotherapy by microneedle patch-assisted delivery of anti-PD1 antibody, Nano Lett. 16 (2016) 2334–2340.

[33] I. Ortega-Oller, M. Padial-Molina, P. Galindo-Moreno, F. O'Valle, A.B. Jódar-Reyes, J.M. Peula-García, Bone regeneration from PLGA micro-nanoparticles, Biomed. Res. Int. 2015 (2015).

[34] B.V. Robinson, F.M. Sullivan, J.F. Borzelleca, S.L. Schwartz, PVP: A Critical review of the kinetics and toxicology of polyvinylpyrrolidone (Povidone), Lewis Publishers, Michigan, 1990.

[35] T.R.R. Singh, I.A. Tekko, F.A. Shammari, A.A. Ali, H. McCarthy, R.F. Donnelly, Rapidly dissolving polymeric microneedles for minimally invasive intraocular drug delivery, Drug Deliv. Transl. Res. 6 (2016) 800–815.

[36] S. Freitas, H.P. Merkle, B. Gander, Microencapsulation by solvent extraction/evaporation: reviewing the state of the art of microsphere preparation process technology, J. Control. Release. 102 (2005) 313–32.

[37] L. Vora, V.G. Sita, P. Vavia, Zero order controlled release delivery of cholecalciferol from injectable biodegradable microsphere: In-vitro characterization and in-vivo pharmacokinetic studies, Eur. J. Pharm. Sci.107 (2017) 78-86

[38] A. Alsaqr, M. Rasoully, F.M Musteata, Investigating transdermal delivery of Vitamin D_3. AAPS PharmSciTech. 16 (2015) 963–972.

[39] T. Ramezanlia, B.E. Kilfoylea, Z. Zhang, B.B. Michniak-Kohn, Polymeric nanospheres for topical delivery of vitamin D_3. Int. J. Pharm. 516 (2017) 196-203.

[40] A. Ripolin, J. Quinn, E. Larrañeta, E.M. Vicente-Perez, J. Barry, R.F. Donnelly, Successful application of large microneedle patches by human volunteers, Int. J. Pharm. 521 (2017) 92–101.

[41] R.F. Donnelly, K. Moffatt, A.Z. aid Alkilani, E.M. Vicente-Pérez, J. Barry, M.T.C. McCrudden, A.D. Woolfson, Hydrogel-forming microneedle arrays can be effectively inserted in skin by self-application: a pilot study centred on pharmacist intervention and a patient information leaflet, Pharm. Res. 31 (2014) 1989–1999.

[42] A.C. Anselmo, S. Mitragotri, An overview of clinical and commercial impact of drug delivery systems, J. Control. Release. 190 (2014) 15–28.

Figure Legends.

Fig. 1. Schematic representation of fabrication of PLGA nano-microparticle-loaded bilayer microneedle arrays.

Fig. 2. Particle size and particle size distribution of VD_3-loaded PLGA NMP preparation (A) without 5% w/w mannitol and (B) with 5% w/w mannitol. Redline (-) indicates the bimodal distribution of particle size from nano- to micron size.

Fig. 3. *In-vitro* release study of VD_3 from PLGA NMP prepared with and without 5% w/w mannitol (Means ±S.D., n =3).

Fig. 4. Digital microscopic images of PLGA NMP-loaded bilayer microneedles. (A) Conical MN arrays (19×19). (B) Conical arrays (12×12). (C) Pyramidal (14×14) arrays.

Fig. 5. Customisation of the height of bilayer structure of microneedle arrays based on the different ratio of NMP and microneedle-forming polymer (PVP). Digital microscopic images of MN prepared from the different weight ratios of NMP and PVP. (A) 1:1, (B) 1:1.5, (C) 1:2, (D) 1:2.5 and (E) 3D graph based on calculated heights of bilayer structure with different weight ratios of NMP and PVP. The needle heights are the average obtained after measuring at least 10 needles per array in 4 different MN arrays.

Fig. 6. Scanning electron micrograph of PLGA NMP-loaded bilayer microneedles: (A) Single array images of conical microneedles; i) Single needles from 19×19 arrays; ii) Single needles from 12×12 arrays. (B) Cross section of a single needle of : i) 19×19 arrays ii) 12×12 arrays and (C) i) Microneedles from pyramidal arrays ii) Single needle from pyramidal arrays.

Fig.7. Percentage of holes created in each Parafilm M® layer and their corresponding insertion depth, using an insertion force of 32 N for bilayer microneedles (conical) arrays (means ± S.D., n = 3) (A). Percentage reduction in height of MN (conical) upon exertion a force of 32 N at 1.19 m/s, held for 30 s (means ± S.D., n = 3) (B).

Fig. 8. Optical coherence tomography images after insertion of drug-loaded PLGA NMP embedded bilayer microneedle arrays into (A) 8 layers of Parafilm M® (B) full thickness neonatal porcine skin. The dashed line represents the surface of the Parafilm M® /skin.

Fig. 9. The concentration of VD_3 in different depths of excised neonatal porcine skin following the application of control patches and bilayer microneedles containing VD_3-loaded PLGA NMP. Results represent means ± S.D., n =3.

Figure 1

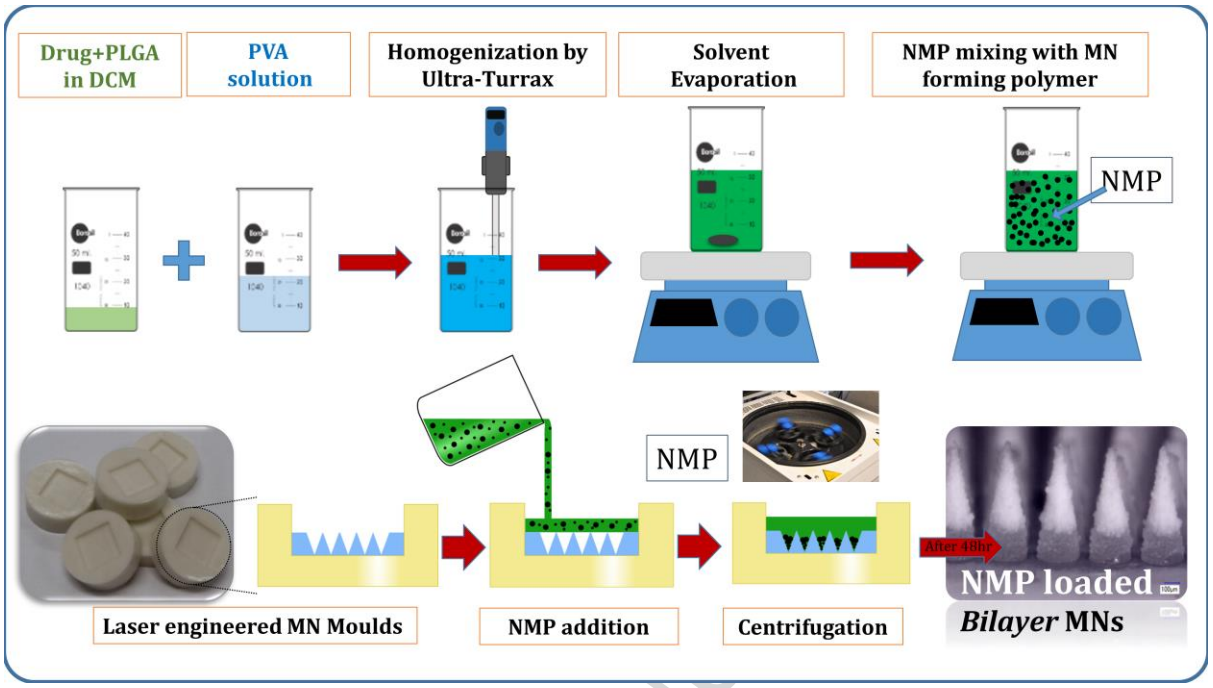

Figure 2

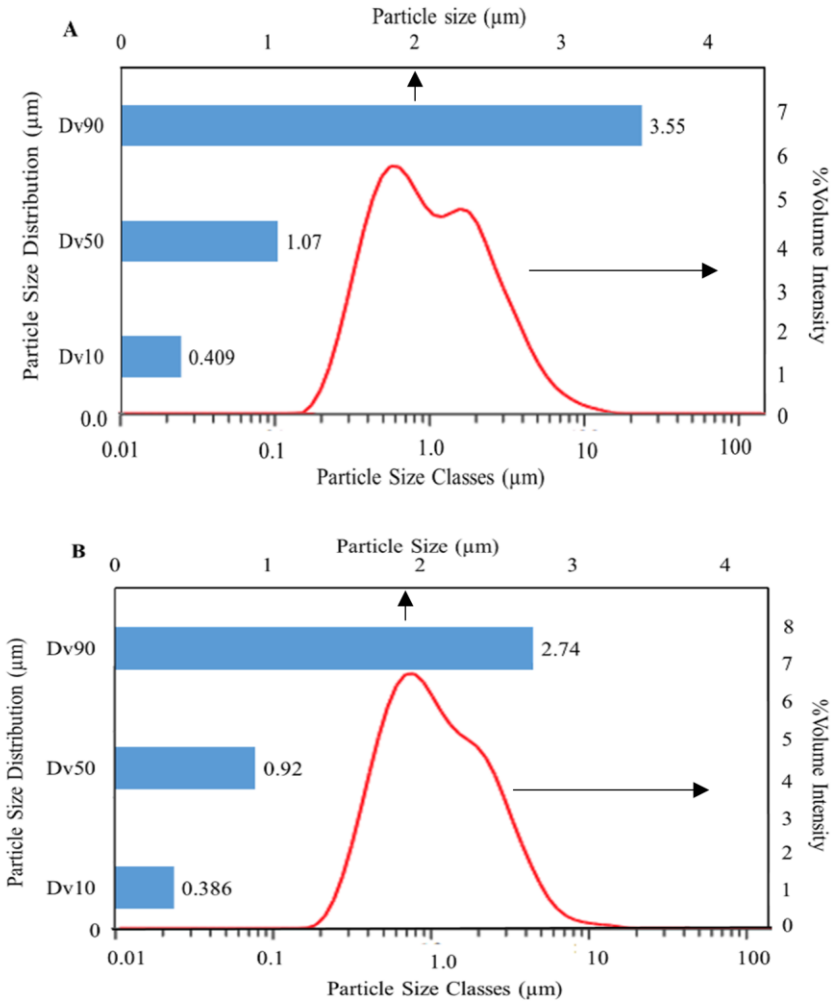

Figure 3

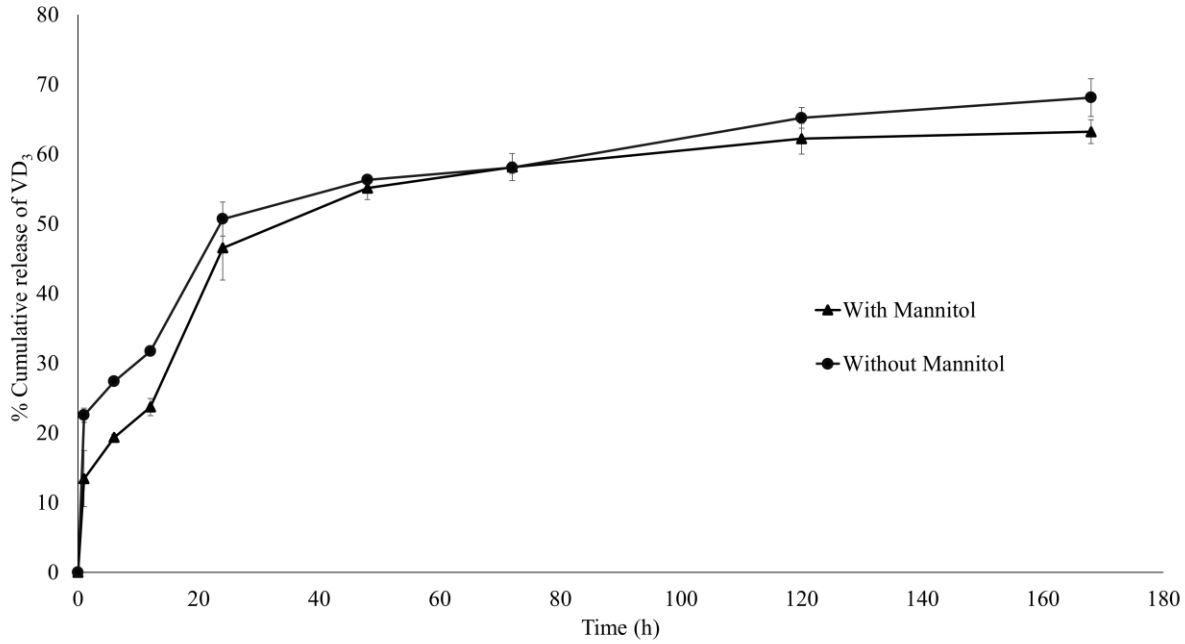

Figure 4

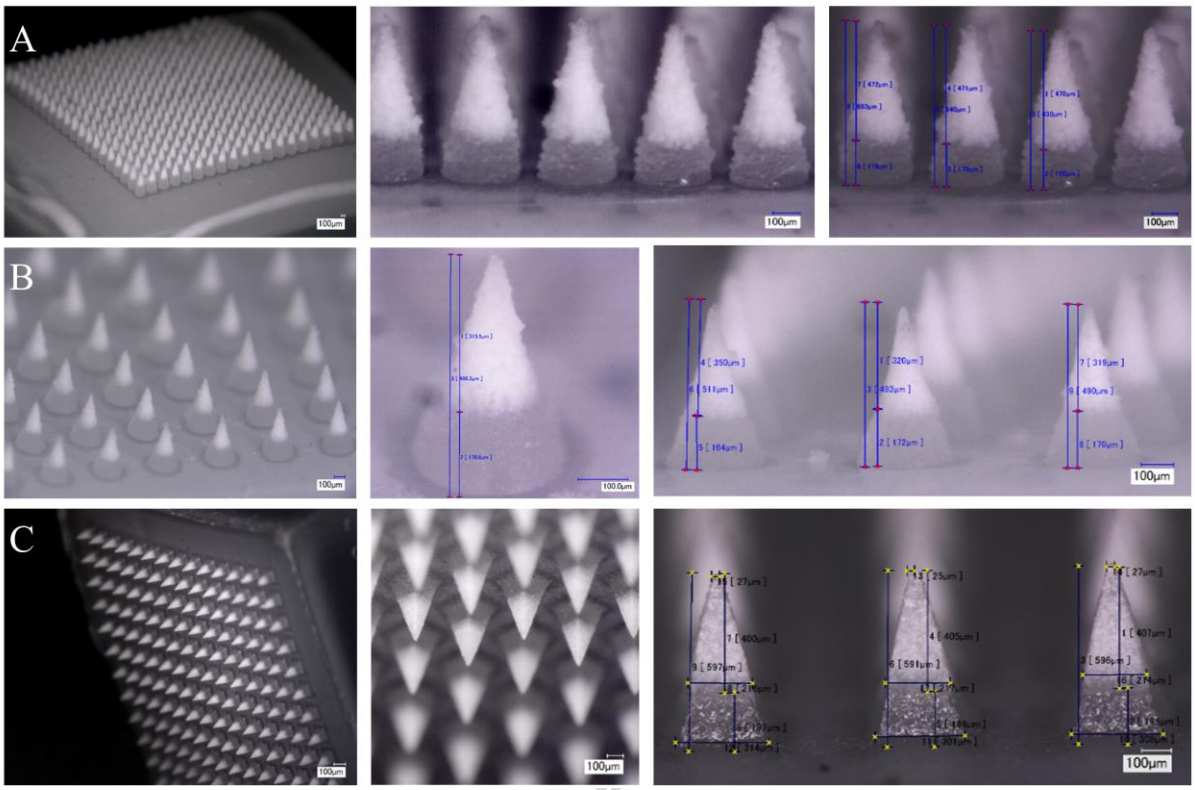

Figure 5

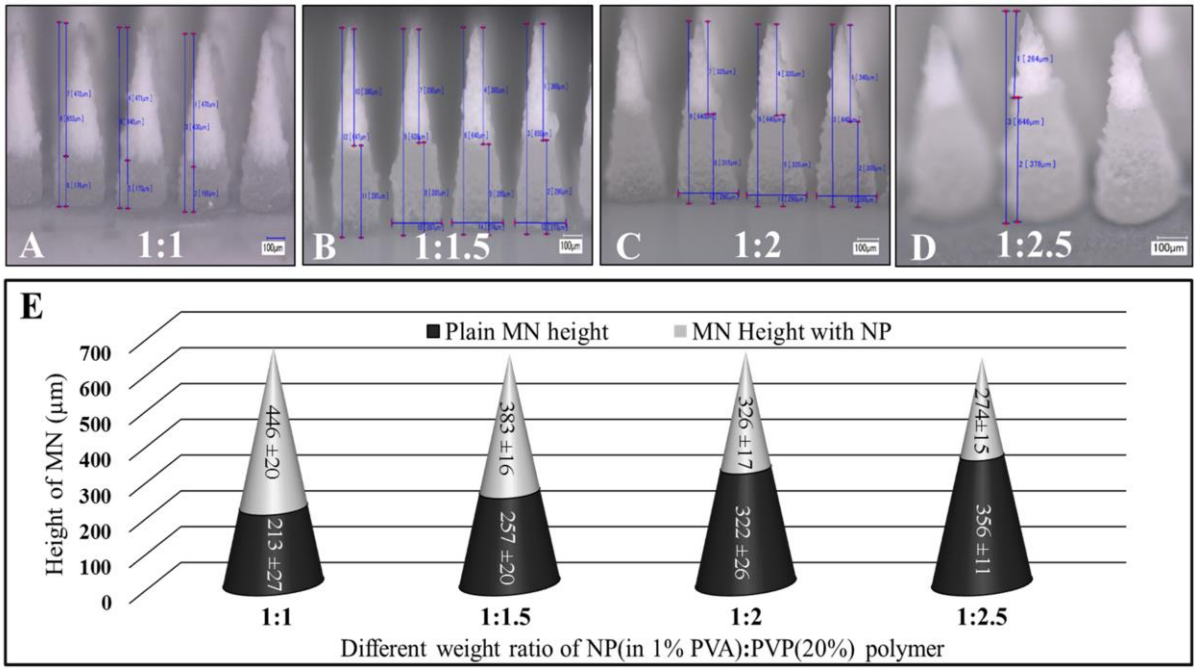

Figure 6

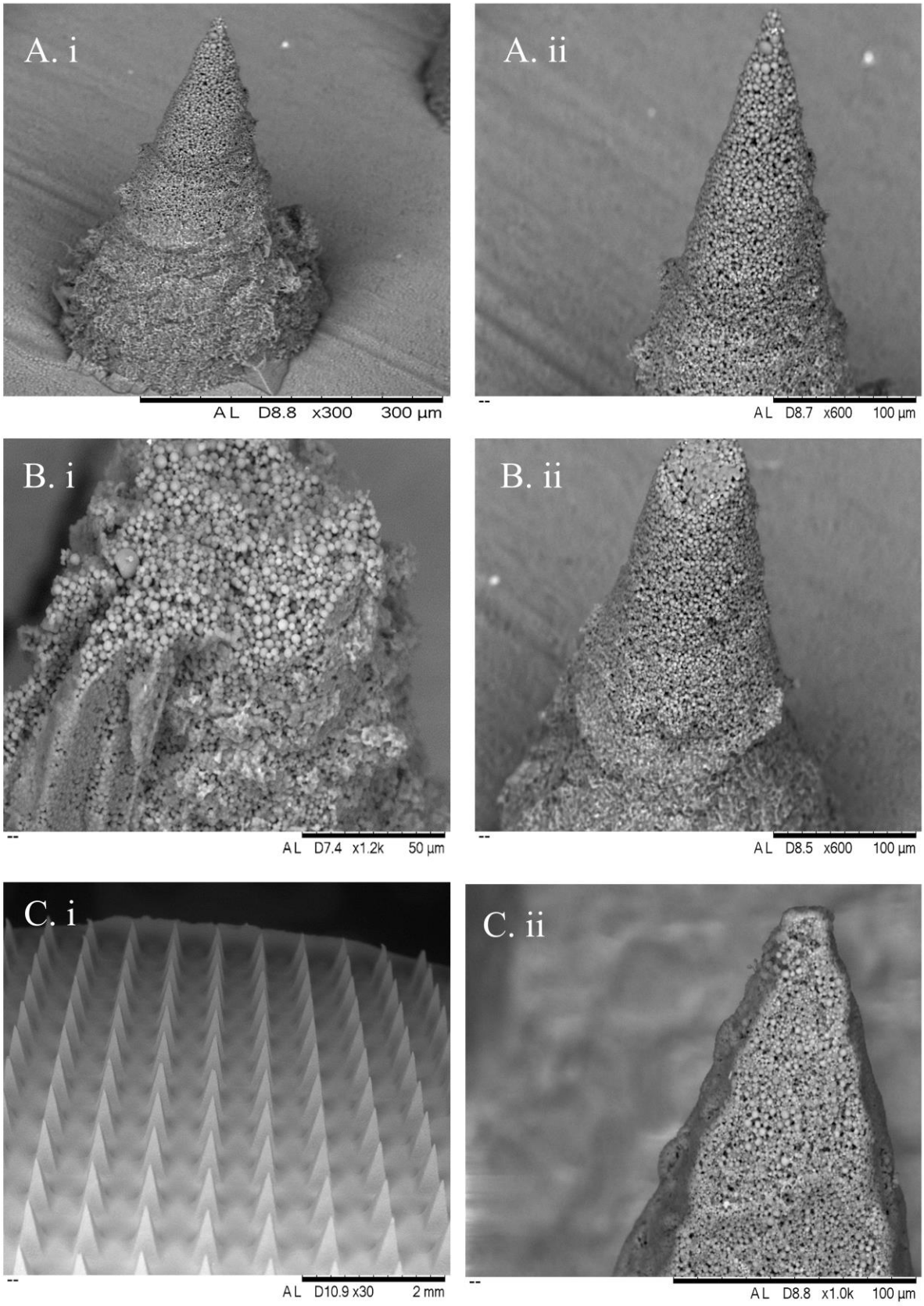

Figure 7

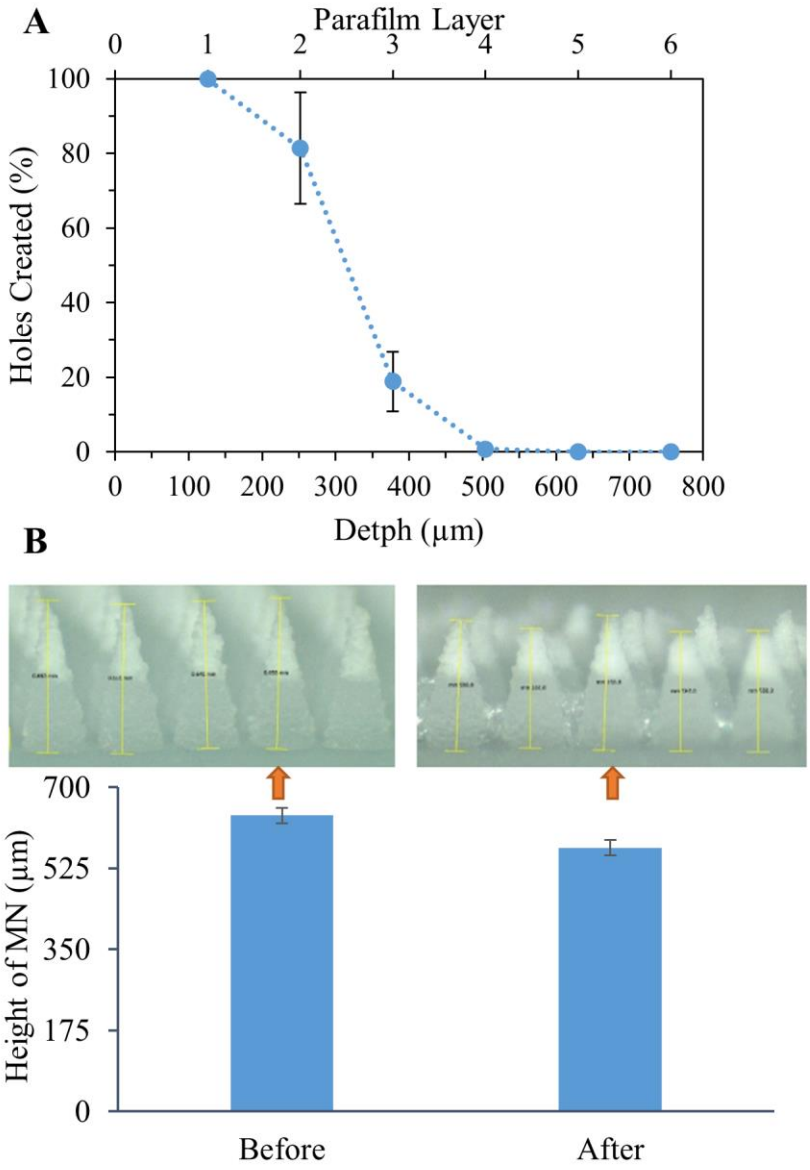

Figure 8

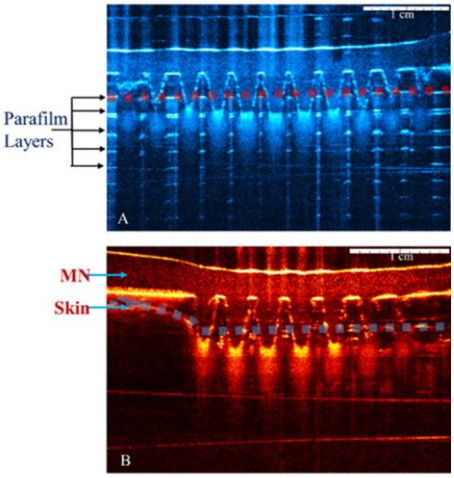

Figure 9

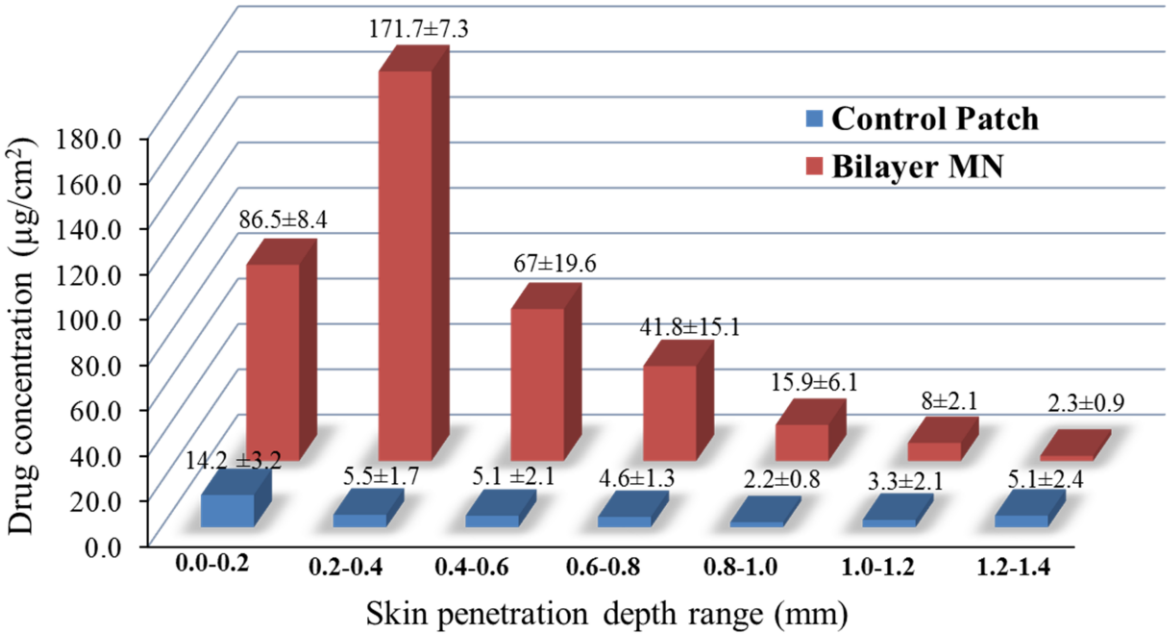

Tables

Table 1 Different ratios of PLGA NMP and 20% PVP solution for microneedle formulation.

Wt Ratio of NMP : PVP	**1:1**	**1:1.5**	**1:2**	**1:2.5**
Solution of NMP	3gm	1gm	1gm	1gm
20% PVP solution	3gm	1.5gm	2gm	2.5gm

Table 2 Particle size and span value of VD_3 loaded PLGA NMP before and after MN formulation

Parameter	**Particle Size**				
	D(0.1)	D(0.5)	D(0.9)	Vol. Weighted Mean D[4, 3]	Span Value
Before MN	286nm	833 nm	2.73 µm	1040nm	2.863
After MN	338nm	843 nm	3.00µm	1095nm	3.156

Graphical abstract